Effects of Shape Change due to Wear on the Accuracy of Vortex-Shedding Flow Meters

Ernst von Lavante, Udo Banaszak
Institute of Turbomachinery, University of Essen, Essen, Germany

Marie Lefebvre
ICAM, Toulouse, France

Abstract - In the present investigation, the problem of accurate determination of volumetric flows by means of the so-called vortex-shedding flowmeter in the case of shape changes from the original specifications due to wear was studied. To this end, the flow about the bluff body used in the presently studied vortex-shedding flow meter was numerically simulated using a solver of the unsteady, compressible Navier-Stokes equations in two and three dimensions. The computations were carried out for several Reynolds numbers using modified geometry in which rounded edges representing wear were introduced. The results were compared, where possible, with experimental data obtained by the manufacturer. The effects of turbulence were modeled by using the realizable k-ε turbulence model. The resulting flow fields were analyzed using various methods, including visualization, evaluation of several of their global features and DFT of properly chosen variables.

Keywords: Vortex Flow Meters, Flow Simulation, Accuracy

1. INTRODUCTION

Many chemical and environmental processes found in the corresponding industries require volume- or mass flow data for their completion. Number of promising new methods for flow rate measurement have been recently developed. One relatively simple flow measurement device is the so-called vortex-shedding flow meter, in which the volumetric flow is determined by observing the relationship between the vortex-shedding frequency from a bluff body attached inside a channel, and the corresponding mean velocity about it. The bluff body causes production of a system of periodic vortices (vortex street), whose frequency can be correlated with the mean flow velocity and, therefore, the volumetric flow. This procedure assumes a regular and well defined vortex structure as well as shedding mechanism, resulting mostly in linear dependency of the volumetric flow on the shedding frequency over a wide range of Reynolds numbers.

Commercial flow meters use a large variety of bluff body shapes, often restricted by the attachment of the pressure sensors or, more likely, the patent laws. In the past, various shapes of vortex bodies have been tested with regard to their applicability to a simple signal processing. Triangular shapes (Johnson [4], Fureby [1]and Madabhushi et. al. [5]) as well as shapes with truncated tips (e. g. Hans et. al. [2] and [3]) have been tested. Previous application of some currently manufactured bluff body designs lead to fairly irregular signals detected by various means, making the determination of the flow rate unreliable. The signal quality was improved by bluff bodies designed specifically for supressing secondary flow phenomena (von Lavante et al. [6]), giving excellent measurement results. It has been also observed that a slight uncontrolled modification of the assumed geometry of a particular vortex-shedding flow meter, e.g. shape, location relative to the surrounding casing and change of shape due to wear caused by particles suspended in the metered fluid, could cause a shift of its characteristic frequencies, leading to unreliable volumetric flow data. The influence of the manufacturing tolerances on the accuracy of vortex-shedding flow meters has been investigated in [7] by von Lavante et al. The effects caused by the abrasion are the subject of the present investigation. This time, only compressible gas (air) at atmospheric conditions was assumed to be the metered fuid.

2. PRINCIPLE OF VORTEX-SHEDDING FLOWMETERS

In principle, the vortex-shedding flowmeters use the separation frequency of vortices behind a bluff body to measure the mean flow velocity of a fluid flow. Downstream of the bluff body, a von Karman vortex street develops; its width d and distance T between the vortices depends on this frequency, and therefore on the bluff body's shape. Preferably, the vortex-shedding frequency should depend linearly on the mean flow velocity for a wide Reynolds number range. The dependency of the vortex frequency f, the mean flow

velocity u_m and the width of the bluff body d is expressed by the dimensionless Strouhal number Sr:

$$Sr = (d \cdot f)/u_m.$$

For a proper operation of the meter, the Strouhal number has to be constant over a wide range of Reynolds numbers. Usually, the detection of the vortices is carried out by pressure sensors inside the bluff body. The vortex structures can also be detected by an ultrasound barrier behind the body, as implemented by, for example, Hans et al. [2].

The present flow meter is using rather a simple method of detecting the vortices shed by the bluff body. A second much smaller body was installed behind the main bluff body, protruding from the wall almost to the centre of the meter. The meter correlates the frequency of oscillation of the bending moment exerted on this paddle to the flow rate. The main advantage of this arrangement is its integrating characteristic (it measures the integral of the pressure on its surface), resulting in a rather smooth signal, as can be seen in Fig. 7. The geometry as considered in the present work is displayed in Fig. 2. Here, the outer casing (piping) has been removed in order to show the shape and position of the bluff body and the paddle. The test section selected for the present studies had a diameter of 50 mm (DN50).

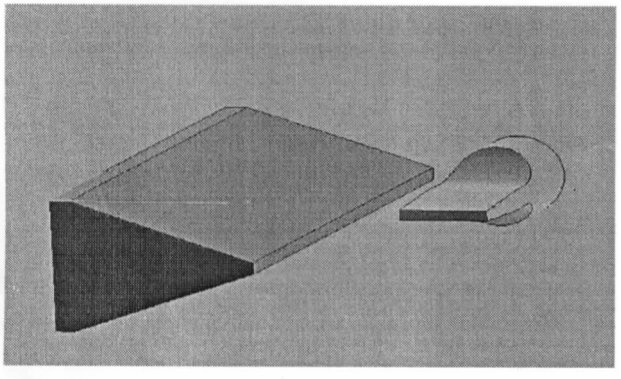

Figure 2. Geometry of the bluff body and paddle used for measuring the vortex-shedding frequency.

3. NUMERICAL METHOD

In the present work, the flow was investigated using a commercially available Navier-Stokes equations solver, the FLUENT system of programs Version 6.xx, capable of handling unsteady, compressible and incompressible viscous flows over a wide range of applications. In all simulations, the realizable k-ε turbulence model was applied.

Close attention was paid to the formulation of the inflow and outflow boundary conditions, as these had to be perfectly nonreflective. The best results were obtained in the case of compressible flows using either the pressure far-field or the pressure inlet boundary condition in the inflow and the pressure outlet boundary in the outflow. All the other boundary conditions available in FLUENT gave inferior results. In particular, the widely used velocity inlet boundary condition, which specifies rigidly the velocity at the inflow, resulted in a perfectly steady flow! In the case of incompressible flow, the above boundary conditions can not be used. Here, the velocity specifying inlet boundary had to be selected. As this boundary condition is perfectly reflecting, something had to be done in order to avoid spurious waves being trapped in the computational domain. The authors had to devise a „dump" region of high numerical viscosity far downstream of the bluff body to damp out these waves.

The standard fully developed turbulent velocity profile due to Nikuradse found in, for example, Schlichting [8], was implemented at the inflow boundary. The so called segregated solver was used in its second-order accurate implicit form. The computations were compared with global experimental results consisting mainly of very accurately measured vortex shedding frequency.

4. BASIC CONFIGURATION

Since a typical fully three-dimensional simulation of the configuration shown in Fig. 2 requires in excess of 10^6 cells and therefore several computational weeks, it was decided to first investigate the present problem in two dimensions. The two-dimensional configuration assumed in the present work can be seen in Fig. 3. It consists of a projection of the bluff body and the paddle, oriented downstream of it.

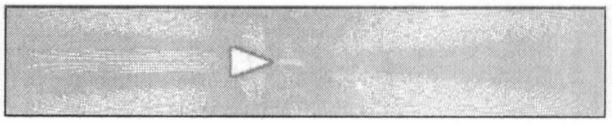

Fig. 3. Basic configuration studied.

A structured computational grid consisting of more than 40 000 cells arranged in 10 blocks was generated. Close attention was paid to the grid resolution in critical areas such as boundary layers. A part of the grid about the two bodies is displayed in Figure 4 for the basic configuration according to the designer's plans.

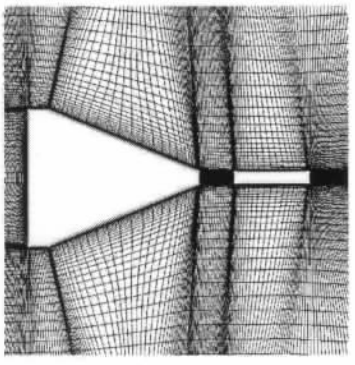

Fig. 4. Partial view of the computational grid for the basic configuration.

Even in the two-dimensional case, the convergence to the correct solution required several days on a 2 GHz PC. A momentary static pressure distribution for the maximum volumetric flow given by u_m= 65 m/s can be found in Fig. 5. At this mean velocity, the Reynolds number was Re=$57 \cdot 10^3$ based on the bluff body hight. Here, the pressure is displayed as gauge pressure in Pa relative to the ambient pressure of 10^5 Pa. Recognizable is not only a strong primary vortex just passing over the paddle, but also a secondary vortex on the top of the rear portion of the bluff body. As the typical von Karman vortex street develops, this secondary vortex alternates between the upper and lower surfaces of the bluff body.

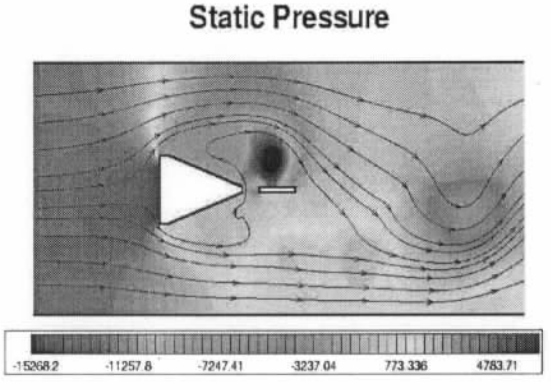

Fig. 5. Static pressure and streamlines at the bluff body and the paddle.

Interestingly, there is a fairly strong flow in direction perpendicular to the main flow between the two bodies. A further primary vortex is just passing out of the view.

The computed unsteady force in vertical direction (called from now on lift) on the paddle (second body) is shown in Fig 7. In this and all the subsequent figures, the lift force is shown in N/m since the flow was assumed to be two.dimensional. The predicted lift displays satisfyingly regular shape. The results of a DFT-transformation using the Hanning filter can be viewed in Fig.8 in the frequency domain. Accordingly, the lift displays a clean peak in the frequency domain, Fig. 8.

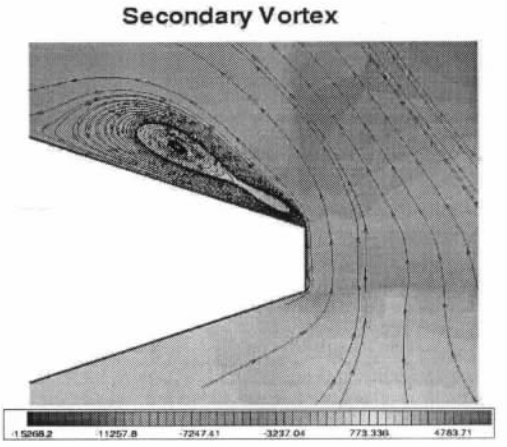

Fig. 6. Secondary vortex on the bluff body.

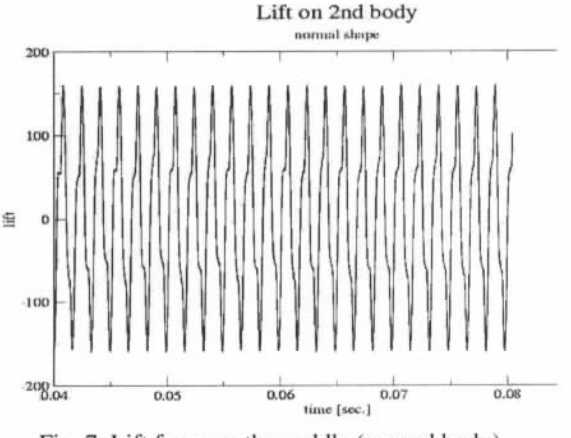

Fig. 7. Lift force on the paddle (second body).

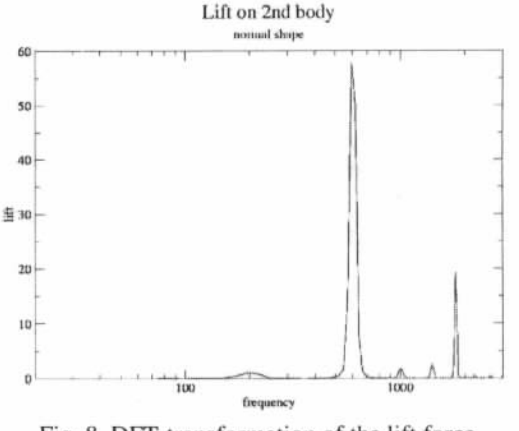

Fig. 8. DFT-transformation of the lift force.

The resulting dominating frequency of 593 Hz agrees rather well with the measured frequency of 590 Hz. The corresponding Strouhal Number is Sr=0.1220, being within 0.5% of the measured value. The present two-dimensional simulation was not able to recover the degree of linearity measured experimentally. This is to be expected, since the assumed shape in Fig. 3 is trying to model the configuration in Fig. 2. The paddle extends in reality approximately to the centerline, causing at its tip

severe three-dimensional effects.

The dependency of the Strouhal number Sr on the Reynolds number Re can be viewed in Fig. 14. For larger Reynolds numbers and, therefore, mean velocities the Strouhal number remains constant within approximately 2.5 %, which is again in good agreement with the experiments. At the smallest Reynolds number, corresponding to an inflow velocity of about u_m= 33 m/s, the assumption of compressible flow is at its limits. In particular, the inflow boundary condition is strictly valid only for compressible flows, e.g. for Mach numbers in access of approximately M=0.15.

5. Three-dimensional Results

As explained above, significant three-dimensional effects were expected to occure in the presently studied meter due to the asymmetric paddle. Therefore, in order to be able to asses their importance, a fully three-dimensional simulation was carried out. The corresponding grid consisted of approximately 4.8 10^5 cells arranged in 31 blocks. Again, as in the case of the two-dimensional simulations, the grid was structured, with very high resolution at locations with significant gradients of the flow variables.

The resulting velocity field is displayed at one instant on a plane cutting through the flow field at approfimately 1/4 diameter from the opposite channel wall in figure 9.

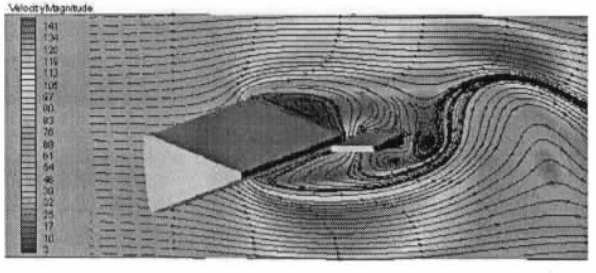

Fig. 9. Velocity contours on a surface of the three-dimensional configuration.

Here, the red countours of the total velocity magnitude correspond to the highest velocity of approximately 145 m/s, while the dark blue contours represent zero velocity.

The flow accelerates strongly around the leading edges of the bluff body, seen as red contour. On the upper surface, one of the primary vortices is forming. The second body (paddel) causes noticable disturbance, seen as vortical structure behind it.

The computed frequency of the lift fluctuation on the paddle, obtained for three different volumetric flows, agreed very nearly perfectly with the experimental data, emphasizing the importance of the three-dimensional effects in this configuration. The Strouhal number, plotted as a function of the Reynolds number, can be seen in figure 14 as compared with all the other results of the present and previous work. The agreement with the experimental data as well as the linearity of the three-dimensional results is remarkable.

6. Bluff Body with Rounded Edges

The wear of the meter, caused by impingement of abrasive particles in the metered fluid, was approximated by rounding the edges of the bluff body to a radius of 0.5 mm. The grid used in these simulations is shown in fig. 10, displaying in an insert a detail of the grid at the rounded edge. It consisted of 160 10^3 cells arranged in 12 blocks.

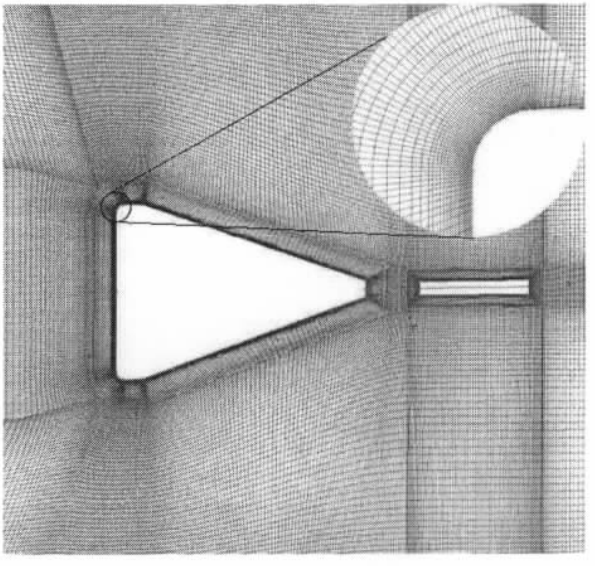

Fig. 10. Computational grid showing the rounded edges.

At mean velocities below 50 m/s, the signal from the paddle was as regular as the one shown in figure 7 for the reference case. However, at higher velocities, the signal became somewhat irregular. A typical example is displayed in Fig. 11 for the mean velocity u_m = 61 m/s.

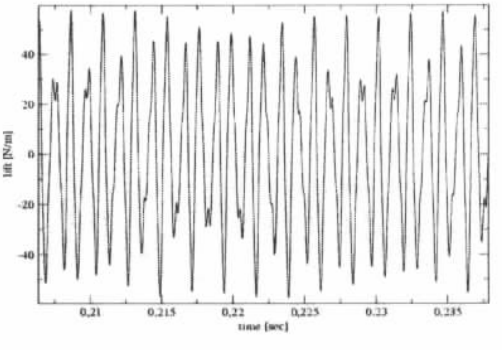

Fig. 11. Lift force on second body, rounded edge.

The flow field offers some rather interesting features. A detailed view of the flow near the two bodies reveals that there is a rather complex structure with several secondary and tertiary vortices. At higher speeds, these vortices interfere with the primary vortices generating the signals shown in figure 11.

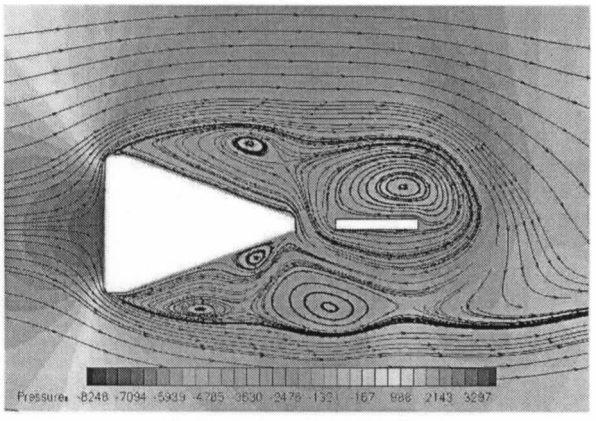

Fig. 12. Static pressure distribution.

The performance (or the lack of it) of the vortex flow meter with the rounded edges at the leading face of the bluff body will be discussed by comparing the signals from this configuration with the basic design configuration. Since the present results were obtained for the two-dimensional case only, they can not be considered quantitatively as compared to the experiments but have to be discussed in relation to the two-dimensional base case.

At flow velocities below 50 m/s, there is no difference in the behavior of the meter between the design bluff body (sharp edges) and the worn bluf body (rounded edges). The signals in the form of lift coefficients on the second body (paddle) depend linearly on the mean flow velocity, as shown in figure 13. At this velocity range, the Strouhal number is constant, as can be seen in figure 14.

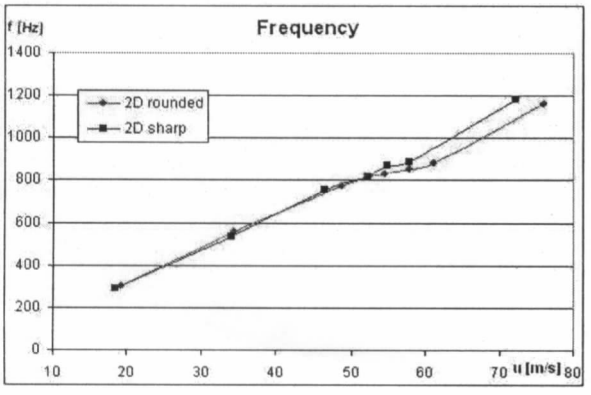

Fig. 13. Results of DFT of the lift force in Fig. 10.

At velocities above 50 m/s, however, the secondary effects become stronger, influencing the lift on the paddle and causing fairly sudden change in the slope of the frequency in figure 13, which results in a change of the Strouhal number. Worse yet - there is not only a jump in the value of the frequency, but also a change of the slope of the linear dependency of the frequency on the velocity.

7. SUMMARY

The present simulations were carried out for a configuration representing a deviation from a preferred design due to wear caused by abrasion by particles suspended in the metered fluid. The resulting Strouhal numbers Sr, shown as a function of the Reynolds number Re based on the height of the bluff body d, are displayed in Fig. 14 as compared with all the other configurations of the present vortex flow meter investigated previously [7].

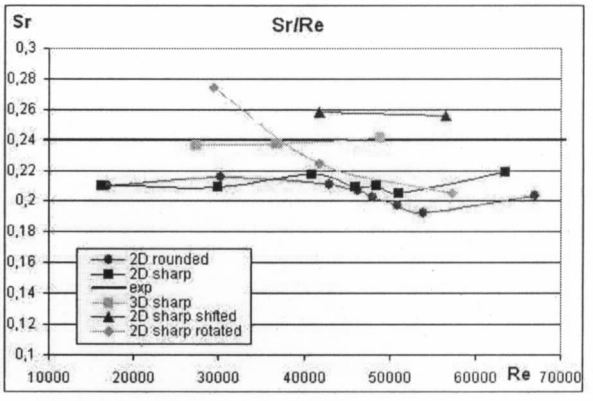

Fig. 14. Strouhal number vs. Reynolds number for different cases as a comparison with the experiment.

Four particular cases should be compared: the experimental data, the three-dimensional results and, in particular, the two-dimensional results for the reference case with infinitely sharp edges with the resulting Strouhal number for the worn bluff body with the rounded edges.

The experimental value is shown as a line, although the measured frequency can differ from the linear relationship by as much as 3 %. As pointed out previously, the three-dimensional results agree surprisingly well with the experiments. The two-dimensional base case displays a fairly good linearity at, however, significanly lower values of the Strouhal number. The Strouhal numbers in the presently studied worn-out meter are essentially the same as for the base case up to a Reynolds number of approximately 45 10^3, after which there is a significant decrease of the vortex shedding frequency cause by secondary flow phenomena. Clearly, this behaviour is very detrimental to the accuracy of the meter. At this time, our recommendation is to replace the bluff body of this meter.

Further research, in particular three-dimensional simulations, are necessary to shed more light on this behaviour.

REFERENCES

[1] C. Fureby, „Large-eddy simulation of turbulent anisochoric flows“, AIAA Journal, Vol. 33, No. 7, pp. 1263-1272, 1995.

[2] Hans, V., Poppen, G., Lavante, E. v., Perpeet, S., „Interaction between vortices and ultrasonic waves in vortex-shedding flow meters“, FLUCOME '97, Hayama, 1997.

[3] Hans, V., Poppen, G., Lavante, E. v., Perpeet, S., „Vortex-shedding flow meters and ultrasound detection: signal processing and bluff body geometry“, Flow Measurement and Instrumentation 9, pp. 79-82, 1998.

[4] Johnson, M.W., „Computation of flow in a vortex-shedding flow meter“, Flow Measurement and Instrumentation, pp. 201-208, 1990 .

[5] Madabhushi, R.K., Choi, D., Barber, T.J., „Unsteady simulations of turbulent flow behind a triangular bluff body“, AIAA Paper, pp. 97-3182, 1997.

[6] von Lavante, E., Yao, J. and Perpeet, S., „Effects of Disturbed Inflow on Vortex-Shedding from a Bluff Body“, AIAA paper 2000-2220, 2000.

[7] von Lavante, E., Nath, B. and Färber, J., "Effects of Manufacturing Tolerances on the Accuracy of Vortex-Shedding Flow Meters", XVII IMEKO World Congress on Metrology, Dubrovnik, 2003.